



Vibration of damaged beams under a moving mass: theory and experimental validation

C. Bilello^{a,*}, L.A. Bergman^b

^a *Dipartimento di Ingegneria Strutturale e Geotecnica, Università degli Studi di Palermo, Viale delle Scienze, Palermo 90128, Italy*

^b *University of Illinois at Urbana-Champaign, 104 S. Wright St., 321E Talbot Lab., MC-236, Urbana, IL 61801, USA*

Received 14 January 2003; accepted 16 June 2003

Abstract

A theoretical and experimental study of the response of a damaged Euler–Bernoulli beam traversed by a moving mass is presented. Damage is modelled through rotational springs whose compliance is evaluated using linear elastic fracture mechanics. The analytical solution is based on the series expansion of the unknown deflection in a basis of the beam eigenfunctions. The latter are calculated using the transfer matrix method, taking into account the effective mass distribution of the beam. The convective acceleration terms, often omitted in similar studies, are considered here for a correct evaluation of the beam–moving mass interaction force.

The analytical solution is then validated through a series of experimental tests. An adequate small-scale model is designed to satisfy both static and dynamic similitude with a prototype bridge structure, thus providing data of practical engineering relevance. It is shown that experimental results are in good agreement with the theoretical predictions. Moreover, it is observed that the percentages of variation in the beam response due to damage are, generally, larger than those induced in the structural natural frequencies; that is, an increase in structural damage sensitivity is noticed under the effect of a moving interacting load.

© 2003 Elsevier Ltd. All rights reserved.

1. Introduction

For more than a century [1] the analysis of continuous elastic systems subjected to moving sub-systems has been a subject of interest in many fields, from structural to mechanical to aerospace engineering. However, it is especially in bridge engineering that this problem finds its widest field of application. Indeed, the presence of structural damage, either due to environmental loads

*Corresponding author. Tel.: +39-091-656-8406; fax: +39-091-656-8407.

E-mail address: bilello@diseg.unipa.it (C. Bilello).

(corrosion, material loss, support deterioration) or to stress concentrations (cracks, joint failures), combined with the dynamic nature of the excitation can dramatically reduce the useful life of the bridge.

In order to recognize when the structure is approaching an overstressed condition, it is necessary to understand the complexity of the dynamic interaction between the continuous system (bridge) and the sub-system (vehicle) moving on it. A complete analysis must also take into account the presence of existing structural damage.

For the undamaged case, a large number of theoretical investigations have been based on use of a beam model; despite its simplicity, it provides useful information for investigating structural response. The complexity of the solution depends on the moving vehicle model. For the simplest moving force model, closed form solutions are available primarily based on the series expansion of the unknown displacement function [2–4]. On the other hand, the so-called moving mass problem, where the inertia of the moving sub-system is taken into account, does not have a closed form solution. Thus, proposed approximate solutions have been based on series expansions [5,6], iterative solution of integral equation [7], and finite element discretization [8,9]. A more complex and realistic model is represented by a moving oscillator [10–12], from which more advanced vehicle models originate [13–16].

Interest in the dynamic analysis of damaged beams has been ongoing for the past 40 years, particularly because of its relationship to the automatic monitoring of structural integrity. A thorough literature survey can be found in Ref. [17].

Basically, damage models presented in the literature can be cast into two categories. The most common, and widely used to study cracked beams, is the so-called “rotational spring model”, in which the effect of structural damage is modelled through a local compliance which quantifies, in a macroscopic way, the relation between the applied load and the strain surrounding the crack area [18–20]. In the most general case a 6×6 local flexibility matrix is introduced whose elements are evaluated using linear elastic fracture mechanics theory [21,22].

Recently, starting from the work of Christides and Barr [23], new continuous vibration theories for cracked beams [24–26] have been developed employing the so-called *crack disturbance functions* that modify the stress, strain, and displacement fields in the entire damaged element. These represent a more advanced and accurate damage model; however, experimental tests and numerical simulations [25,26] have shown that the rotational spring model, despite its simplified assumptions (localized damage effect), provides a good approximation of the beam response.

In spite of the large number of publications focused on the two fields, moving loads on continuous elastic systems and vibration of damaged structures, to the authors’ knowledge only three [27–29] have addressed these two topics simultaneously. In Parhi and Behera [27], the problem of a mass moving on cantilever beam with a single damage location is investigated. In Ref. [28] a procedure is presented for determining stress intensity factors for single and double edge cracks in a simply supported undamped Euler–Bernoulli beam under a moving force; while in Ref. [29] an iterative procedure is proposed for the analysis of the moving mass case. In these papers linear elastic fracture mechanics is used to calculate the compliance of the equivalent rotational spring damage model. However, a number of undocumented assumptions are made, either in the structural model (lumped masses [28,29]) or in the evaluation of the beam–moving mass interaction force (convective acceleration terms are omitted [27]) while the convergence conditions for the iterative scheme in Ref. [29] are not clearly stated. Moreover, the experimental

data in Ref. [27], due to the selected range of variation of parameters governing the problem, do not provide information of significant engineering relevance.

In light of the potential developments in the field of structural health monitoring and damage identification in bridge structures, this problem has become of fundamental importance. Indeed, enormous economic advantages could arise from the use of simple moving load tests for integrity checks in highway bridges.

The first objective of this work, treated in Section 2, is to provide an analytical tool for the analysis of a damaged Euler–Bernoulli beam under a moving mass, with an arbitrary number of damaged sections, and generic boundary conditions. A rotational spring damage model is used (Section 3). The formulation of the problem, starting from the equation of motion of the single element of the discretized beam, is given in a compact mathematical form, adaptable to computer implementation. Both the structural model and the beam–moving mass interaction force are modelled in the most accurate way by taking into account the effective structural mass distribution and the convective acceleration terms.

Though relatively simple, this model can be used to study the behaviour of a damaged bridge structure subjected to moving vehicles.

Indeed, in the second part of this work (Section 4), an experimental investigation of a small-scale model of a prototype bridge structure is presented. The objective of this section is not only to validate the analytical tools developed, but also to provide data of practical engineering relevance for analyzing the structural damage sensitivity under a moving mass.

2. Theory

2.1. Formulation of the problem

The given beam is discretized into N segments of constant linear mass density ρ , bending stiffness EI (undamaged beam stiffness), and length l_i (Fig. 1). Damping is not considered. The segments are connected together through rotational springs (damaged sections) whose compliances are denoted by c_i . The equation of motion for the i th segment can then be written as

$$\rho \ddot{w}(x_i, t) + EI \partial^4 w(x_i, t) / \partial x^4 = f_i(t) W[\xi_i(t), 0, l_i] \delta[x_i - \xi_i(t)], \quad 0 < x_i < l_i, \quad (1)$$

where $w(x_i, t)$ is the unknown deflection, overdots denote derivatives with respect to the time variable, $f_i(t)$ is the beam–moving mass interaction force, $W(\cdot)$ is a window function, $\delta(\cdot)$ is the Dirac delta function, and $\xi_i(t)$ denotes the location of the moving load at time t (in the local co-ordinate system). The window function is defined as

$$W[\xi_i(t), 0, l_i] = U[\xi_i(t), 0] - U[\xi_i(t), l_i], \quad (2)$$

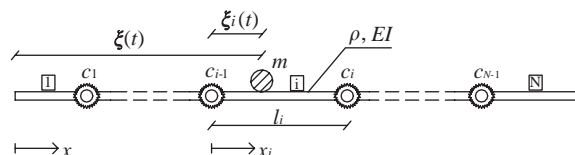


Fig. 1. Beam with rotational springs representing damaged section traversed by a moving mass.

in which $U(\cdot)$ is the unit step function; thus, the right-hand of Eq. (1) is different from zero $\forall t: 0 \leq \xi_i(t) \leq l_i$ (the mass transits over the i th segment).

The expression for $f_i(t)$ depends on the analytical model used to represent the moving load; in the case of a moving mass model it is given by

$$f_i(t) = m\{g - T[w(x_i, t)]|_{x_i=\xi_i(t)}\}, \quad (3)$$

where m is the moving mass, g is the acceleration due to gravity, and $T[\cdot]$ is a linear differential operator for the acceleration of the mass

$$T[\cdot] = \left(\frac{\partial^2}{\partial t^2} + 2\dot{\xi} \frac{\partial^2}{\partial x \partial t} + \dot{\xi}^2 \frac{\partial^2}{\partial x^2} + \ddot{\xi} \frac{\partial}{\partial x} \right) [\cdot]. \quad (4)$$

In this expression $\dot{\xi}$ and $\ddot{\xi}$ are the speed and acceleration of the moving mass, respectively. In a similar study of a single damaged beam under a moving mass [27] the convective terms in Eq. (4) were omitted ($T[\cdot] \cong \partial^2[\cdot]/\partial t^2$); however, this approximation is not generally reasonable unless the mass moves at very low speed, and it may lead to significant errors in the evaluation of the system response.

From Eq. (3) it is apparent that the interaction force depends on the beam response itself; moreover, using Eqs. (3)–(4) in Eq. (1), it is straightforward to show that the governing partial differential equation is characterized by time-varying singular coefficients.

Besides the initial conditions, $w_0(x) = w(x, 0)$ and $\dot{w}_0(x) = \dot{w}(x, 0)$ for $0 \leq x \leq l$ and the external boundary conditions, the interior compatibility and equilibrium relationships must be taken into account in the formulation of the problem; for the case under study they are given by

$$w_i(0, t) = w_{i-1}(l_{i-1}, t), \quad (5a)$$

$$\vartheta_i(0, t) = \vartheta_{i-1}(l_{i-1}, t) + c_{i-1} M_{i-1}(l_{i-1}, t), \quad (5b)$$

$$M_i(0, t) = M_{i-1}(l_{i-1}, t), \quad (5c)$$

$$V_i(0, t) = V_{i-1}(l_{i-1}, t) \quad \text{for } i = 2, 3, \dots, N-1, \quad (5d)$$

where $\vartheta(x, t)$, $M(x, t)$ and $V(x, t)$ denote the slope, bending moment and shear force, respectively. An exact solution of this problem is not, in general, possible. An approximate solution can be obtained by expanding the unknown function $w(x, t)$ in a series of the beam eigenfunctions.

2.2. Eigenvalues and eigenfunctions of the damaged beam

The eigenvalues ω_r and eigenfunctions $\varphi_r(x)$ of the damaged beam are calculated through the *Transfer Matrix Method*. This approach, first introduced by Pestel and Leckie [30], is still an attractive tool for the solution of the eigenvalue problem for one-dimensional systems with non-uniform mechanical properties. Following this approach, for the i th segment of the given Euler–Bernoulli beam (Fig. 2a), the relations between the state at the right- and left-end can

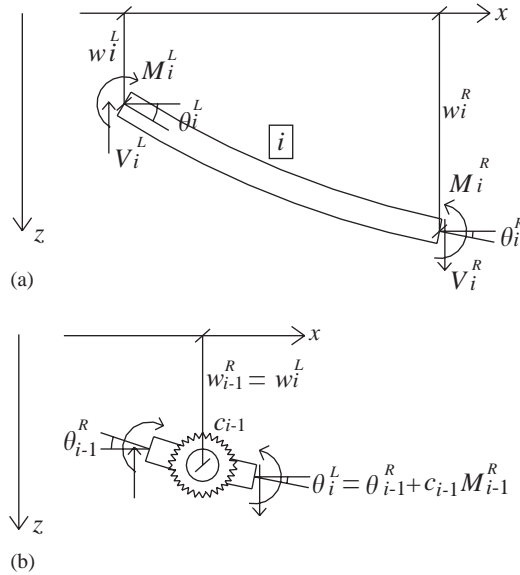


Fig. 2. Beam element: end displacements and forces (a), interior compatibility relations (b).

be written as [30]

$$\begin{bmatrix} -w_i^R \\ \vartheta_i^R \\ M_i^R \\ V_i^R \end{bmatrix} = \begin{bmatrix} t_0(l_i, \gamma) & -t_1(l_i, \gamma) & -\frac{t_2(l_i, \gamma)}{EI} & -\frac{t_3(l_i, \gamma)}{EI} \\ \gamma^4 t_3(l_i, \gamma) & t_0(l_i, \gamma) & -\frac{t_1(l_i, \gamma)}{EI} & \frac{t_2(l_i, \gamma)}{EI} \\ -EI\gamma^4 t_2(l_i, \gamma) & EI\gamma^4 t_3(l_i, \gamma) & t_0(l_i, \gamma) & t_1(l_i, \gamma) \\ EI\gamma^4 t_1(l_i, \gamma) & EI\gamma^4 t_2(l_i, \gamma) & -\gamma^4 t_3(l_i, \gamma) & t_0(l_i, \gamma) \end{bmatrix} \begin{bmatrix} -w_i^L \\ \vartheta_i^L \\ M_i^L \\ V_i^L \end{bmatrix}, \quad (6a)$$

or in compact matrix form

$$\mathbf{z}_i^R = \mathbf{U}_i \mathbf{z}_i^L. \quad (6b)$$

In Eqs. (6) \mathbf{U}_i is the so-called *transfer matrix*, $\gamma^4 = \omega^2 \rho / EI$, and $t_0(x, \gamma)$, $t_1(x, \gamma)$, $t_2(x, \gamma)$ and $t_3(x, \gamma)$ are transcendental functions reported in the Appendix. It is worth noting that in Refs. [28,29], a lumped-mass transfer matrix is used; however, when the number of segments (damaged sections) is relatively small, the lumped-mass model can introduce a significant approximation; unless the undamaged segments are also divided into smaller ones [28,29]. The latter approach is certainly possible but it requires additional computational efforts that can be avoided using the distributed mass transfer matrix.

Using the notation just introduced, the interior compatibility and equilibrium equations (5) are written as (Fig. 2b)

$$\mathbf{z}_i^L = \mathbf{C}_i \mathbf{z}_{i-1}^R \quad \text{for } i = 2, 3, \dots, N - 1, \quad (7a)$$

where C_i is a 4×4 matrix given by

$$C_i = \begin{bmatrix} 1 & 0 & 0 & 0 \\ 0 & 1 & c_{i-1} & 0 \\ 0 & 0 & 1 & 0 \\ 0 & 0 & 0 & 1 \end{bmatrix}. \tag{7b}$$

Thus, starting from the right-end of the beam, all segments are reconnected together so that the following relationship holds:

$$z_N = z_N^R = U_N C_N U_{N-1} C_{N-1} \dots C_1 U_1 z_1^L = A(\omega) z_0. \tag{8}$$

Finally, taking into account the proper boundary conditions, one obtains

$$\hat{A}(\omega) \hat{z}_0 = 0, \tag{9}$$

where $\hat{A}(\omega)$ is 2×2 reduced matrix. The eigenvalues ω_r are the roots of the transcendental equation

$$\det[\hat{A}(\omega)] = 0. \tag{10}$$

Once the eigenvalues have been obtained using any of a number of root-finder algorithms, the beam eigenfunctions, together with their derivatives up to the third order, can be calculated directly from Eqs. (8) and (9). Using Eqs. (7) and the proper boundary conditions, it can be easily shown that the orthonormality relationships for this case are [31–33]

$$\sum_{i=1}^N \int_0^{l_i} \varphi_{is}(x_i) \rho \varphi_{ir}(x_i) dx_i = \delta_{sr}, \tag{11a}$$

$$\sum_{i=1}^N \int_0^{l_i} \varphi_{is}(x_i) EI \varphi_{ir}^{IV}(x_i) dx_i = \omega_s^2 \delta_{sr} \quad \text{for } s, r = 1, 2, \dots, \infty, \tag{11b}$$

where δ_{sr} is the Kronecker delta.

2.3. Dynamic response

The unknown deflection $w(x, t)$ is expanded in a series of the beam eigenfunctions as

$$w(x_i, t) \cong \sum_{r=1}^n \varphi_{ir}(x_i) q_r(t) \quad \text{for } i = 1, 2, \dots, N, \tag{12}$$

in which the approximation is due to the series truncation, and the $q_r(t)$ are unknown time coefficients to be calculated. Using Eqs. (12) and (4) in Eq. (3), the beam–moving mass interaction force is rewritten as (with explicit time omitted)

$$f_i(t) = m \left\{ g - \sum_{r=1}^n \varphi_{ir}(\xi_i) \ddot{q}_r + 2 \dot{\xi} \varphi'_{ir}(\xi_i) \dot{q}_r + [\dot{\xi}^2 \varphi''_{ir}(\xi_i) + \ddot{\xi} \varphi'_{ir}(\xi_i)] q_r \right\}, \tag{13}$$

where the prime denotes differentiation with respect to x .

Operating on Eq. (1) by $\int_0^{l_i} \varphi_{is}(x_i)[\cdot] dx_i$, summing over the N segments, and taking into account the orthonormality relationships (11) yields

$$\ddot{q}_s(t) + \omega_s^2 q_s(t) = F_s(t) \quad \text{for } s = 1, 2, \dots, n, \quad (14)$$

where

$$F_s(t) = \sum_{i=1}^N \int_0^{l_i} \varphi_{is}(x_i) f_i(t) \mathbf{W}[\xi_i(t), 0, l_i] \delta[x_i - \xi_i(t)] dx_i = \sum_{i=1}^N \varphi_{is}[\xi_i(t)] f_i(t) \mathbf{W}[\xi_i(t), 0, l_i]. \quad (15)$$

The right-hand of Eqs. (14) depends on the functions $f_i(t)$ (Eq. (15)) which, in turn, depend on the coefficients $q_r(t)$ (Eq. (13)); it is clear, then, that Eqs. (14) are a set of coupled second order linear differential equations. However, within all the terms of the summation in Eq. (15), only one will be different from zero, i.e., the one for which $\mathbf{W}[\xi_i(t), 0, l_i] = 1$. Thus, to calculate $F_s(t)$ at any time t , one must scan the entire beam to find out which is the loaded segment.

In order to simplify the program implementation and allow for a more succinct presentation of the equations involved, introduce the functions

$$\phi_{r,p}(x) = \sum_{i=1}^N \varphi_{ir}^{(p)}(x - L_{i-1}) \mathbf{W}(x, L_{i-1}, L_i) \quad \text{for } r = 1, 2, \dots, n, \quad (16)$$

where $L_i = \sum_{k=1}^i l_k$ and $L_0 = 0$. These will be called *computational eigenfunctions*. Note that $\phi_{r,p}(x) \neq \phi_r^{(p)}(x)$.

This approach is similar to the one used in Pesterev et al. [34] to study the dynamic response of a beam traversed by a stream of oscillators.

Substituting Eq. (13) into Eq. (15) and following notation (16) yields

$$F_s(t) = m \phi_{s,0}[\xi(t)] \left\langle g - \sum_{r=1}^n \phi_{r,0}[\xi(t)] \ddot{q}_r + 2\dot{\xi} \phi_{r,1}[\xi(t)] \dot{q}_r + \{\dot{\xi}^2 \phi_{r,2}[\xi(t)] + \ddot{\xi} \phi_{r,1}[\xi(t)]\} q_r \right\rangle. \quad (17)$$

Using Eq. (17) one can rewrite the set of Eqs. (14) in a compact matrix form as

$$\mathbf{M}(t) \ddot{\mathbf{q}}(t) + \mathbf{D}(t) \dot{\mathbf{q}}(t) + \mathbf{K}(t) \mathbf{q}(t) = mg \mathbf{\Phi}_0[\xi(t)], \quad (18)$$

where $\mathbf{q}(t)$ is an n -dimensional vector collecting the unknowns $q_r(t)$, $\mathbf{\Phi}_p(x) = [\phi_{1,p}(x), \phi_{2,p}(x), \dots, \phi_{n,p}(x)]$, and the system matrices are given by

$$\mathbf{M}(t) = \mathbf{I}_n + m \mathbf{\Phi}_0^T[\xi(t)] \mathbf{\Phi}_0[\xi(t)], \quad (19a)$$

$$\mathbf{D}(t) = 2m \dot{\xi}(t) \mathbf{\Phi}_0^T[\xi(t)] \mathbf{\Phi}_1[\xi(t)], \quad (19b)$$

$$\mathbf{K}(t) = \mathbf{\Omega}^2 + m \mathbf{\Phi}_0^T[\xi(t)] \{\dot{\xi}^2(t) \mathbf{\Phi}_2[\xi(t)] + \ddot{\xi}(t) \mathbf{\Phi}_1[\xi(t)]\}, \quad (19c)$$

in which \mathbf{I}_n is an n -dimensional identity matrix and $\mathbf{\Omega}^2 = \text{diag}[\omega_1^2, \omega_2^2, \dots, \omega_n^2]$.

The initial conditions associated with Eq. (18) are written as

$$\mathbf{q}(0) = \int_0^l \mathbf{\Phi}_0^T(x) \rho w_0(x) dx; \quad \dot{\mathbf{q}}(0) = \int_0^l \mathbf{\Phi}_0^T(x) \rho \dot{w}_0(x) dx. \quad (20a - b)$$

Due to the interaction between the beam and the mass moving on it, all of the system matrices in Eq. (18) are time dependent. As already mentioned, in a number of previous studies, an approximation to the interaction force has been used so that $\mathbf{D} \equiv \mathbf{0}$ and $\mathbf{K} \equiv \mathbf{\Omega}^2$; however, as can

be seen from Eqs. (19b)–(19c), these matrices depend on the speed and the acceleration of the moving mass. It can be shown that, at high speeds or under significant acceleration, the approximation leads to an underestimation of the structural response. Thus, for certain types of structures (for example bridges for high-speed railways, decks for aircraft carriers), especially in the presence of damage, the correct interaction force is necessary for accurate response prediction.

The set of equations (18) can be solved using any of a number of numerical integration schemes. The solution procedure presented has been implemented in a Matlab[®] code. Once the vector $\mathbf{q}(t)$ has been obtained, one can calculate the beam response according to the expressions

$$w(x, t) = \Phi_0^T(x)\mathbf{q}(t), \quad (21a)$$

$$\vartheta(x, t) = \Phi_1^T(x)\mathbf{q}(t), \quad (21b)$$

$$M(x, t) = -EI\Phi_2^T(x)\mathbf{q}(t), \quad (21c)$$

$$V(x, t) = -EI\Phi_3^T(x)\mathbf{q}(t). \quad (21d)$$

It is worth noting that, for $\mathbf{M} \equiv \mathbf{I}_n$, $\mathbf{D} \equiv \mathbf{0}$ and $\mathbf{K} \equiv \Omega^2$ in Eq. (18), the moving force solution is obtained. Finally, the procedure just described can easily be extended to include the case in which each segment of the beam differs in stiffness and mass density.

3. Damage model

The rotational spring model has been shown to lead to reasonable predictions of the static as well as the dynamic behaviour of damaged beams [18–22,25,26]. Though it has been used mainly to model cracked beams, experimental tests [33] have shown that, for simpler problems (beam under a bending load, stable damage size), the spring model can also be applied to model saw-cuts. However, it should be clearly stated that, to avoid the introduction of non-linearity in the structural model, the saw-cut is assumed to remain open during vibration. This hypothesis has been successively verified and confirmed by the experimental tests.

The damage configuration used for the experiments presented in the next section is shown in Fig. 3. Damage is realized through symmetric saw-cuts with a depth equal to a . The beam

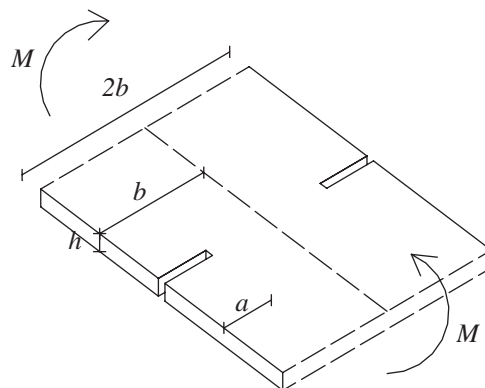


Fig. 3. Damage and load configuration.

cross-section has height h and width $2b$. To the authors' knowledge, the equivalent compliance corresponding to this damage and load configuration was not available in the literature. Thus, following the classical approach based on linear elastic fracture mechanics, taking into account the effective stress distribution throughout the cut depth [21,35], the compliance can be expressed as [33]

$$c = \frac{6\pi}{Eh^3} \int_0^\beta \bar{y} F^2(\bar{y}) d\bar{y}, \quad \bar{y} = y/b, \quad \beta = a/b, \quad (22a)$$

where

$$F(\bar{y}) = \frac{1.122 - 0.561\bar{y} - 0.205\bar{y}^2 + 0.471\bar{y}^3 - 0.190\bar{y}^4}{\sqrt{1-\bar{y}}}. \quad (22b)$$

Eqs. (22) have been used for all numerical simulations herein.

4. Experimental validation

The analytical solution has been validated through experimental tests performed on a small-scale model of a prototype bridge structure. Details of the similitude requirements set forth by a proper dimensional analysis are reported in Bilello et al. [36]. It is remarkable that, under simplified assumptions (Euler–Bernoulli beam model), both static and dynamic similitude requirements have been satisfied; attention has been paid in particular to the satisfaction of the mass similitude, often constituting one of the main difficulties in the design of small-scale dynamic models.

Thus, the experimental model has been designed to provide results of practical engineering relevance.

4.1. Experimental model

The model used in the experimental investigation [33,36] consists of a 6061 T-6 aluminum beam with dimensions $1071.5 \times 105.25 \times 6.35$ mm. Two 1.25 mm diameter steel rods were glued to the model to form a rail that is used to guide the mass moving on it (Fig. 4). The weight of the beam, including the rail, is 19.79 N, corresponding to a linear mass density ρ equal to 184.7×10^{-8} N s² mm⁻². The bending stiffness, estimated from preliminary static tests, is $EI = 162.6 \times 10^6$ N mm².

The beam is simply supported at both ends along two pre-machined lines 10 mm from the end edges. The left-end support is fixed while the right-end support is carried by a linear ball bearing slide. A triangular tip is mounted on the top surface of each support, and the beam rests on it. A thin film of machine oil is applied on the supporting lines to reduce the friction as much as possible. Each support is connected to a rigid aluminum plate that, in turn, is bolted to a rigid concrete block. A plywood ramp is placed next to the model for the acceleration of the moving mass. A thin aluminum layer forms its rolling surface on which is glued the same rail as in the model. The inclination of the surface is 60°. The ramp stands on three adjustable feet that allow levelling with the beam. The moving mass is a 4.952 N steel disk, whose diameter and thickness

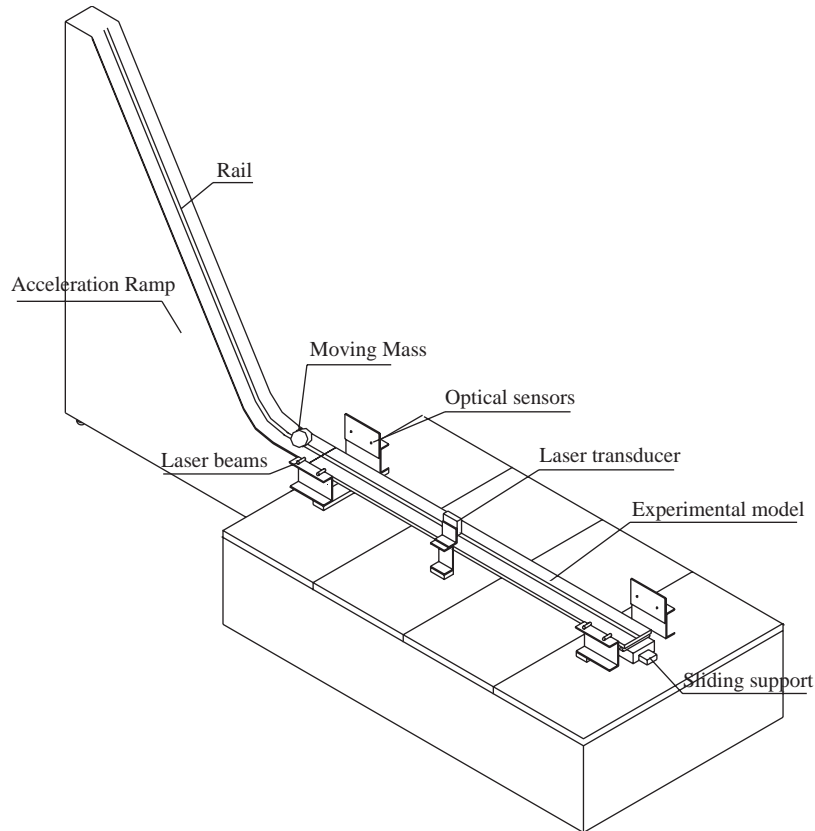


Fig. 4. Experimental model and set-up.

are, respectively, 50.8 and 38.1 mm. The disk is pre-machined so that it rolls on the rail glued to the ramp and beam.

4.2. *Experimental set-up*

Four optical diodes are used to measure the entrance and the exit speed of the moving disk. They are mounted in couples, spaced 50.8 mm apart, on aluminum supports located at the two ends of the model. The output signal from the left-end side diode is used to trigger the test.

The beam deflection is measured through a laser displacement transducer focused on a point 460 mm (7/16*l*) from the left-end support. The output signals are acquired through an A/D board integrated with a Tektronix 2630 spectrum analyzer. No windows are applied to the signals; they are directly stored and then processed.

The experimental model has been used for static as well as impact hammer and moving mass tests. Four configurations have been investigated: undamaged model, damaged Level 1, damaged Level 2, and damaged Level 3 (Table 1). The number of tests performed, for each speed range and each model configuration, varied from 30 to 100 depending on the difficulties encountered in the

Table 1
Damaged model configurations

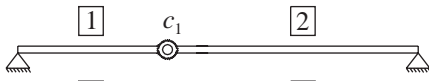

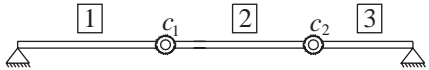
Notation	Damage location	Damage extent $\beta = a/b$	Structural model
Level 1	6/16l	0.3	
Level 2	6/16l	0.6	
Level 3 = Level 2+	12/16l	0.6	

Table 2
Averages and standard deviations of the disk entrance speeds and decelerations

Test	Experimental model		Prototype structure		Exp. and prot.	
	$E[v]$ (km/h)	$\sigma[v]$ (km/h)	$E[v]$ (km/h)	$\sigma[v]$ (km/h)	$E[a]$ (m/s ²)	$\sigma[a]$ (m/s ²)
V1	3.06	0.05	23.10	0.37	-0.07	0.012
V2	4.12	0.08	31.08	0.59	-0.10	0.022
V3	4.63	0.06	34.93	0.48	-0.10	0.025
V4	5.18	0.07	39.11	0.56	-0.12	0.033
V5	5.72	0.09	43.16	0.65	-0.14	0.046
V6	6.35	0.09	47.92	0.65	-0.16	0.052
V7	6.92	0.10	52.25	0.78	-0.17	0.075
V8	7.59	0.13	57.31	1.01	-0.17	0.099

repeatability of the experiments. The tests were labeled V1–V8 to distinguish between the eight entrance speeds.

The average and standard deviation of the entrance speeds and decelerations are reported in Table 2. It is worth noting that the disk deceleration is reasonably small. The speed range goes from $v \approx 3$ km/h ($v \approx 23$ km/h in the prototype scale) to a maximum of $v \approx 7.6$ km/h ($v \approx 60$ km/h in the prototype scale). Larger values could not be obtained without risking damage to the experimental set-up. Nevertheless, this range is sufficient to represent realistic vehicle speeds.

4.3. Results

Preliminary static tests have been performed to validate the damage model. The results of these tests are reported in Table 3 in terms of identified damage. Good agreement can be observed, confirming the validity of the damage model. These identified values of damage extent (rotational spring compliance) have been used in the successive numerical analysis.

In Table 4 the first six theoretical and experimental natural frequencies (obtained from impact hammer tests) are compared. Note that, for the model configurations Levels 1 and 2, damage is located in the vicinity of a node of the third mode shape (5.33/16l); thus, the corresponding natural frequency is nearly unchanged. The theoretical results agree very well with the

Table 3
Comparison between experimental and identified damage extents

Damage configuration	Damage extent $\beta = a/b$	
	Effective	Identified
Level 1	0.3	0.287
Level 2	0.6	0.562
Level 3 = Level 2+	0.6	0.592

Table 4
Comparison between theoretical and experimental frequencies (Hz)

	Undamaged		Damaged Level 1		Damaged Level 2		Damaged Level 3	
	Theor.	Exp.	Theor.	Exp.	Theor.	Exp.	Theor.	Exp.
f_1	13.322	13.507	13.231	13.233	12.963	13.007	12.743	12.896
f_2	53.291	52.965	53.078	52.560	52.478	52.147	50.623	50.840
f_3	119.90	118.41	119.76	118.44	119.36	117.87	117.49	116.53
f_4	213.16	210.58	211.48	209.60	206.97	205.54	206.95	205.17
f_5	333.07	334.41	332.68	330.99	331.68	328.34	325.82	324.85
f_6	479.62	479.60	477.73	471.60	472.68	464.52	459.71	453.98

experimental ones. The maximum absolute error is equal to 1.726% (f_6 for damage Level 2) while the maximum difference between the undamaged and damaged measured fundamental frequencies is equal to 4.52%.

Some results of the moving mass tests are reported in Fig. 5. The theoretical solution is compared with the average measured one. It has been observed that the experimental response is basically due only to the first mode; thus, a digital Butterworth low-pass filter with a cut-off frequency $f_c = 30$ Hz has been applied to the data to remove unwanted high-frequency content which does not affect the maximum response. In the light of this consideration, the theoretical response has been calculated retaining only the first term of the series expansion (12).

The experimental results agree very well with the theoretical ones in terms of trend and maximum deflection (Table 5). In general the experimental response is larger than the calculated one and, after the peak, it shows higher response than the theoretical one. This may be caused by out-of-plane oscillations of the moving disk that, in turn, can be due to rolling surface irregularities or small deviations of the rail-guide from a straight line. The maximum absolute error between theoretical and the experimental results is 5.32%, while the maximum difference between the damaged and undamaged measured deflection is 11.37% (damage level 3 V6).

It should be noted that the deflection increases with damage level but not always with the moving disk's speed (for the experimental as well as the theoretical data); moreover, the percentages of variation in the beam response to the moving mass are larger than those induced in the beam dynamic parameters. Thus, a higher structural sensitivity is observed under the effect of a moving interacting load.

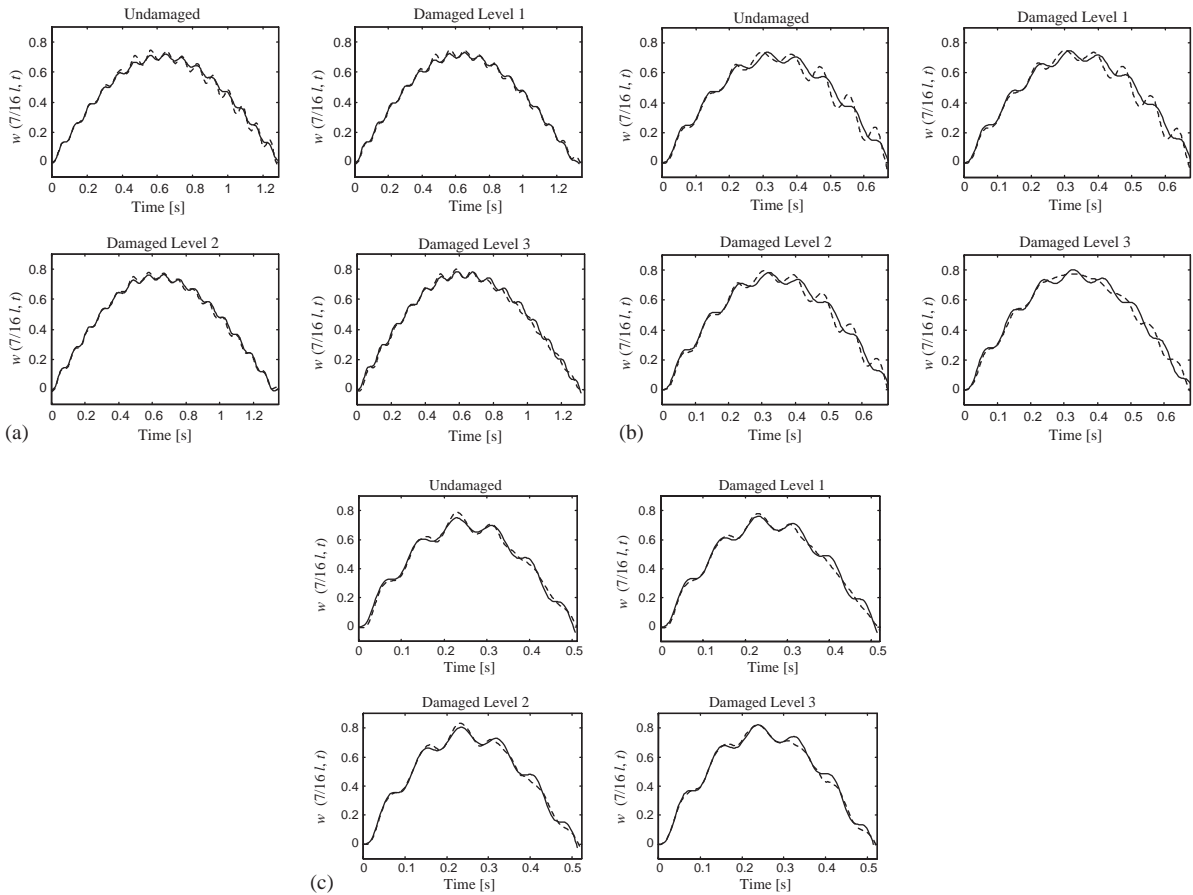


Fig. 5. (a) Theoretical (solid line) and experimental (dashed line) beam deflection versus crossing time for different model configurations at section $x = 7/16l$: entrance speed V1. (b) Theoretical (solid line) and experimental (dashed line) beam deflection versus crossing time for different model configurations at section $x = 7/16l$: entrance speed V5. (c) Theoretical (solid line) and experimental (dashed line) beam deflection versus crossing time for different model configurations at section $x = 7/16l$: entrance speed V8.

Table 5
Comparison between maximum theoretical and experimental deflection (mm)

	Undamaged		Damaged Level 1		Damaged Level 2		Damaged Level 3	
	Theor.	Exp.	Theor.	Exp.	Theor.	Exp.	Theor.	Exp.
V1	0.729	0.747	0.730	0.746	0.764	0.777	0.784	0.799
V2	0.726	0.756	0.738	0.763	0.773	0.801	0.783	0.787
V3	0.730	0.736	0.741	0.737	0.779	0.791	0.799	0.797
V4	0.729	0.770	0.742	0.767	0.775	0.814	0.790	0.796
V5	0.736	0.739	0.747	0.751	0.783	0.794	0.802	0.775
V6	0.743	0.712	0.754	0.733	0.788	0.764	0.806	0.793
V7	0.732	0.743	0.742	0.747	0.789	0.812	0.808	0.801
V8	0.749	0.787	0.761	0.779	0.804	0.832	0.821	0.821

Finally, it should be noted that these experimental observations can be directly extended, through proper scale factors [36], to the prototype structure.

5. Conclusions

A procedure for the analysis of damaged Euler–Bernoulli beams under a moving mass, with an arbitrary number of damaged sections and generic boundary conditions, is presented. The analytical solution is based on the series expansion of the unknown deflection in the basis of the beam eigenfunctions; the latter properly account for the presence of internal rotational springs representing damaged sections.

Taking into account the convective terms of the beam–moving mass interaction force leads to a set of second order linear differential equations with time varying coefficients (mass, damping and stiffness) which governs the given problem. Computational eigenfunctions are introduced for a concise formulation of the problem and to accommodate computer implementation.

The analytical solution is validated through experimental tests on a small-scale model designed to satisfy both static and dynamic similitude with a prototype bridge. It is shown that experimental results are in good agreement with theoretical predictions. The experimental response often appears to be larger than the calculated one.

Moreover, it is observed that the presence of damage results in larger perturbations (in percentage) to the dynamic response to a moving load rather than to the dynamic properties of the damaged element itself. Thus, an increase in structural damage sensitivity is noticed under the effect of a moving interacting load.

Since experimental tests are performed on a scaled model of a bridge prototype structure, the experimental results assume practical engineering relevance in light of the potential developments in the field of structural health monitoring and damage identification in bridge structures.

Acknowledgements

The financial support of the US National Science Foundation, through Grant number CMS-9800136, which made the experimental investigation reported in this paper possible, is gratefully acknowledged.

Appendix

The transcendental functions used for the definition of the transfer matrix \mathbf{U}_i in Eqs. (6) are given by

$$t_0(x, \gamma) = \frac{1}{2}(\cos \gamma x + \cosh \gamma x), \quad (\text{A.1a})$$

$$t_1(x, \gamma) = \frac{1}{2\gamma}(\sin \gamma x + \sinh \gamma x), \quad (\text{A.1b})$$

$$t_2(x, \gamma) = \frac{1}{2\gamma^2}(\cos \gamma x - \cosh \gamma x), \quad (\text{A.1c})$$

$$t_3(x, \gamma) = \frac{1}{2\gamma^3}(\sin \gamma x - \sinh \gamma x). \quad (\text{A.1d})$$

References

- [1] G.G. Stokes, Discussion of a differential equation relating to the breaking of railway bridges, *Transactions of the Cambridge Philosophical Society* 8 (1849) 707–735 Reprinted in *Mathematical and Physical Papers* (1883) (2) 178–220.
- [2] L. Meirovitch, *Analytical Methods in Vibrations*, MacMillan, London, 1967.
- [3] L. Fryba, *Vibration of Solids and Structures under Moving Mass*, Noordhoff, Groningen, 1972.
- [4] A.V. Pesterev, B. Yang, L.A. Bergman, C.A. Tan, Revisiting the moving force problem, *Journal of Sound and Vibration* 261 (2003) 75–91.
- [5] M.M. Stanisic, J.A. Euler, S.T. Montgomery, On a theory concerning the dynamic behavior of structures carrying moving mass, *Ingenieur Archives* 43 (1974) 295–305.
- [6] A.V. Pesterev, L.A. Bergman, A contribution to the moving mass problem, *Journal of Vibration Acoustics* 120 (1998) 824–826.
- [7] S. Sadiku, H.H.E. Leipholz, On the dynamics of elastic systems with moving concentrated mass, *Ingenieur Archives* 57 (1987) 223–242.
- [8] J.E. Akin, M. Mofid, Numerical solution for response of beam with moving mass, *Journal of Structural Engineering* 115 (1987) 120–131.
- [9] M. Mofid, M. Shadam, On the response of beams with internal hinges, under moving mass, *Advances in Engineering Software* 31 (2000) 323–328.
- [10] A.V. Pesterev, L.A. Bergman, Vibration of elastic continuum carrying moving linear oscillator, *Journal of Engineering Mechanics* 123 (1997) 878–884.
- [11] A.V. Pesterev, L.A. Bergman, Vibration of elastic continuum carrying accelerating oscillator, *Journal of Engineering Mechanics* 123 (1997) 886–889.
- [12] B. Yang, C.A. Tan, L.A. Bergman, Direct numerical procedure for solution of moving oscillator problems, *Journal of Engineering Mechanics* 126 (2000) 462–469.
- [13] P. Swannel, C.W. Miller, Theoretical and experimental studies of a bridge–vehicle system, *Proceeding of Institute of Civil Engineering* 83 (1987) 613–635.
- [14] J.L. Humar, A.M. Kashif, Dynamic response of bridges under traveling loads, *Canadian Journal of Civil Engineers* 20 (1993) 287–298.
- [15] P.K. Chatterjee, T.K. Datta, C.S. Surana, Vibration of continuous bridges under moving vehicles, *Journal of Sound and Vibration* 169 (1994) 619–632.
- [16] Y.B. Yang, J.D. Yau, Vehicle–bridge interaction element for dynamic analysis, *Journal of Structural Engineering* 123 (1997) 1512–1518.
- [17] A.D. Dimarogonas, Vibration of cracked structures—a state of the art review, *Engineering Fracture Mechanics* 55 (1996) 831–857.
- [18] G.R. Irwin, Analysis of stresses and strains near the end of a crack traversing a plate, *Journal of Applied Mechanics* 24 (1957) 361–364.
- [19] J.R. Rice, N. Levy, The part-through a surface crack transversing an elastic plate, *Journal of Applied Mechanics* 39 (1972) 185–194.
- [20] A.D. Dimarogonas, *Vibration Engineering*, West Publishers, St. Paul, MN, 1976.
- [21] N. Anifantis, A. Dimarogonas, Stability of columns with a single crack subjected to follower and vertical loads, *International Journal of Solids Structures* 19 (1983) 281–291.

- [22] C.A. Papadopoulos, A.D. Dimarogonas, Coupled longitudinal and bending vibrations of a rotating shaft with an open crack, *Journal of Sound and Vibration* 117 (1987) 81–93.
- [23] S. Christides, A.D.S. Barr, One-dimensional theory of cracked Bernoulli–Euler beams, *International Journal of Mechanical Science* 26 (1984) 639–648.
- [24] M.-H.H. Shen, C. Pierre, Natural modes of Bernoulli–Euler beams with symmetric cracks, *Journal of Sound and Vibration* 138 (1990) 115–134.
- [25] T.G. Chondros, A.D. Dimarogonas, Vibration of a cracked cantilever beam, *Journal of Vibration and Acoustics* 120 (1998) 742–746.
- [26] T.G. Chondros, A.D. Dimarogonas, J. Yao, A continuous cracked beam vibration theory, *Journal of Sound and Vibration* 217 (1997) 17–34.
- [27] D.R. Parhi, A.K. Behera, Dynamic deflection of a cracked shaft subjected to moving mass, *Transactions of the CSME* 21 (1997) 295–316.
- [28] M.A. Mahamoud, Stress intensity factors for single and double edge cracks in a simple beam subjected to a moving load, *International Journal of Fracture* 111 (2001) 151–161.
- [29] M.A. Mahamoud, M.A. Abou Zaid, Dynamic response of a beam with a crack subject to a moving mass, *Journal of Sound and Vibration* 256 (2002) 591–603.
- [30] E.C. Pestel, F.A. Leckie, *Matrix Methods in ElastoMechanics*, McGraw-Hill, London, 1983.
- [31] T. Hayashikawa, N. Watanabe, Dynamic behavior of continuous beams with moving loads, *Journal of the Engineering Mechanics Division* 107 (1981) 229–246.
- [32] J. Lee, L.A. Bergman, The vibration of stepped beams and rectangular plates by an elemental dynamic flexibility method, *Journal of Sound and Vibration* 171 (1994) 617–640.
- [33] C. Bilello, Theoretical and experimental investigation on damaged beams under moving loads, Ph.D. Thesis, Università degli Studi di Palermo, Palermo, 2001.
- [34] A.V. Pesterev, B. Yang, L.A. Bergman, C.-A. Tan, Response and stress calculation of an elastic continuum carrying multiple oscillators, in: J.M. Ko, Y.L. Xu (Eds.), *Proceedings of the International Conference on Advances in Structural Dynamics*, Hong Kong, Dec. 13–15, 2000, Vol. 1, Elsevier, Amsterdam, 2000, pp. 545–552.
- [35] H. Tada, P.C. Paris, G.R. Irwin, *The Stress Analysis and Cracks Handbook*, Del Research Corporation, Hellertown, PA, 1985.
- [36] J.C. Bilello, L.A. Bergman, D. Kuchma, Experimental investigation of a small scale bridge model under a moving mass, *Journal of Structural Engineering* 130 (2004) 799–804.